

# Ultrafast Dynamics of the Carbonyl Stretching Vibration in Acetic Acid in Aqueous Solution Studied by Sub-Picosecond Infrared Spectroscopy

Motohiro Banno,<sup>†</sup> Kaoru Ohta,<sup>‡</sup> and Keisuke Tominaga<sup>\*,†,‡,§</sup>

Molecular Photoscience Research Center, Kobe University, Graduate School of Science and Technology, Kobe University, and CREST/JST, Rokkodai-cho 1-1, Nada, Kobe 657-8501, Japan

Received: August 29, 2007; In Final Form: February 1, 2008

Vibrational energy relaxation of the carbonyl CO stretching modes of CH<sub>3</sub>COOD and CD<sub>3</sub>COOD in D<sub>2</sub>O is studied by frequency-resolved infrared pump–probe spectroscopy. The spectral change caused by the vibrational excitation includes two dynamical components with the time constants of 450 and 980 fs for CH<sub>3</sub>COOD and 390 and 930 fs for CD<sub>3</sub>COOD. The two dynamical components exhibit different spectral properties. There are two species of acetic acid forming different complexes with solvent water molecules. The time constants are almost the same for CH<sub>3</sub>COOD and CD<sub>3</sub>COOD, suggesting that the vibrational energy deposited to the carbonyl group is first distributed among vibrational modes not related to the methyl group.

## 1. Introduction

Aqueous solutions are important chemical reaction fields in nature. When a solute has electron lone pairs, hydrogen bonds are formed between these groups and solvent water molecules. Strong interaction by the hydrogen bonds should influence the static and dynamic environments around the solute molecules in aqueous solution. Therefore, it is essential to acquire deeper information on the hydrogen-bonding dynamics between solute and solvent.

Time-resolved infrared (IR) spectroscopy has been applied to studies of vibrational dynamics in aqueous solution. The vibrational population dynamics of anions, such as N<sub>3</sub><sup>−</sup>, OCN<sup>−</sup>, SCN<sup>−</sup>, and Fe(CN)<sub>6</sub><sup>4−</sup>, in aqueous solution have been investigated with this method.<sup>1–11</sup> In these systems, the vibrational energy relaxation (VER) was characterized by a single time constant, *T*<sub>1</sub>. The vibrational dynamics of *N*-methylacetamide and peptides have also been studied in aqueous solution.<sup>12</sup> The VER process of the carbonyl CO stretching modes of these compounds proceeds with two different time constants of several hundreds of femtoseconds and a few picoseconds. The origin of the two components is not yet understood completely.

Acetic acid is one of the simplest molecules containing a carbonyl group. The structures of acetic acid in aqueous solution have been experimentally investigated with IR,<sup>13,14</sup> Raman,<sup>15–18</sup> and ultraviolet (UV)<sup>19</sup> spectroscopic methods. They have also been studied theoretically.<sup>14,20</sup> These studies have revealed that acetic acid forms hydrogen bond complexes, such as several kinds of dimers and linear-chain oligomers, in concentrated aqueous solution. In contrast, it was concluded that the carbonyl group of acetic acid forms hydrogen bonds predominantly with water molecules in dilute aqueous solution, resulting in the formation of hydrogen-bonded complexes of acetic acid and water.<sup>13,19</sup>

The vibrational dynamics of acetic acid have been studied extensively by time-resolved IR spectroscopy. In particular, the

vibrational dynamics of the CO stretching mode,<sup>21</sup> the OH stretching mode,<sup>22–28</sup> and the OH bending mode<sup>24</sup> of the acetic acid cyclic dimer have been studied, and the results yielded information on the anharmonic coupling between the intramolecular vibrational mode and the low-frequency modes of the hydrogen bonds. The anharmonic coupling of the dimer was also studied theoretically.<sup>25,29</sup> On the other hand, the solute–solvent interaction and the vibrational dynamics of acetic acid in dilute aqueous solution have not yet been studied in detail. In this study, we investigated the vibrational dynamics of the CO stretching mode of CH<sub>3</sub>COOD and CD<sub>3</sub>COOD in dilute D<sub>2</sub>O solution. Observation of the CO stretching vibrational dynamics is useful in order to elucidate the hydrogen-bonding dynamics of solute–solvent complexes. We also compared the results for CH<sub>3</sub>COOD and CD<sub>3</sub>COOD to study the contributions of the methyl group to the inter- and intramolecular vibrational energy transfer from the excited CO stretching mode.

## 2. Experimental Section

A time-resolved IR pump–probe spectrometer was constructed to observe vibrational dynamics. The schematic diagram of the apparatus is shown in Figure 1a. A portion of a Ti:sapphire laser output (300 mW, 1 kHz) was introduced to a home-built optical parametric amplifier (OPA), based on ref 30. A mid-IR pulse was generated by difference frequency mixing between the two near-IR outputs from the OPA in a AgGaS<sub>2</sub> crystal. The mid-IR pulse was divided into three by a CaF<sub>2</sub> wedged window. The 92% of the energy passing through the window was used as a pump pulse, the 4% reflected by the front side of the window was used as a probe pulse, and the remaining 4% reflected by the back side was used as a reference pulse. The pump pulse traversed an optical delay line. The pump and probe pulses were focused on the sample. After passing through the sample, the probe pulse was dispersed by a spectrograph and was detected by a liquid-nitrogen-cooled 32-channel MCT array detector. The reference pulse was also dispersed by the spectrograph and was detected by another array detector. The intensity fluctuations of the probe pulses were corrected by the reference pulses. The relative polarization angle

\* Corresponding author.

<sup>†</sup> Molecular Photoscience Research Center, Kobe University.

<sup>‡</sup> Graduate School of Science and Technology, Kobe University.

<sup>§</sup> CREST/JST.

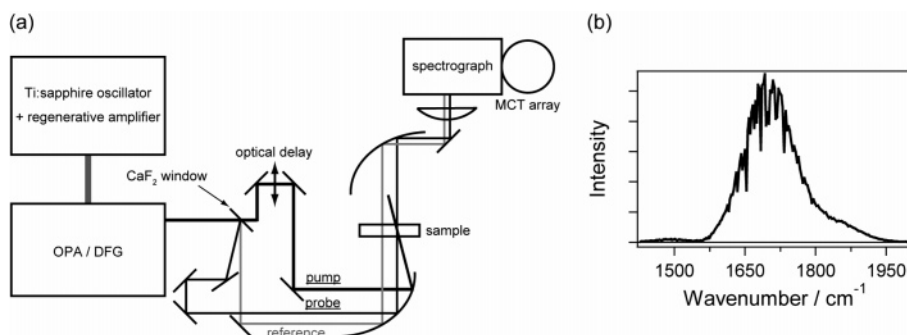


**Figure 1.** Apparatus for time-resolved IR pump–probe spectroscopy. (a) Schematic diagram of the time-resolved IR spectrometer. (b) Spectrum of IR laser light.

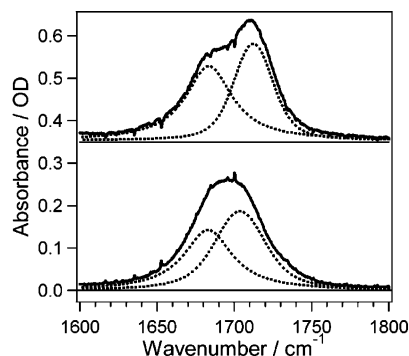


**Figure 2.** Steady-state IR absorption spectra (solid lines) of  $\text{CH}_3\text{COOD}$  (top) and  $\text{CD}_3\text{COOD}$  (bottom) in  $\text{D}_2\text{O}$ . The dotted lines are decomposed Voigt components from each absorption band.

between the pump and the probe radiations was set to the magic angle,  $54.7^\circ$ , by a set of  $\text{CaF}_2$  polarizers and a  $\text{MgF}_2$  half wave plate.

In this study, the wavenumber of the IR light was set to  $1700\text{ cm}^{-1}$ , corresponding to the energy gap between the  $\nu = 0$  and the  $\nu = 1$  states of the carbonyl CO stretching mode of acetic acid in  $\text{D}_2\text{O}$ . The IR pulse energy was about  $1.3\ \mu\text{J}$ . The spectrum of the IR light was measured with a single MCT detector while scanning the output wavenumber from the spectrograph. The recorded spectrum is displayed in Figure 1b. The spectral width was approximately  $160\text{ cm}^{-1}$ . The spectrum covered the entire range of the absorption band of the CO stretching vibration, which is discussed in section 3.1. The temporal resolution of the apparatus was approximately 250 fs, which was estimated from the temporal duration of a nonresonant pump–probe signal from neat  $\text{D}_2\text{O}$ .<sup>12</sup>

$\text{D}_2\text{O}$  solutions of  $\text{CH}_3\text{COOD}$  and  $\text{CD}_3\text{COOD}$  were prepared by dissolution of  $(\text{CH}_3\text{CO})_2\text{O}$  and  $\text{CD}_3\text{COOD}$  into  $\text{D}_2\text{O}$ , respectively. The concentrations of the solutions were  $0.3\text{ mol dm}^{-3}$ . The sample was injected into a  $50\ \mu\text{m}$  thick cell with two  $\text{CaF}_2$  windows.  $(\text{CH}_3\text{CO})_2\text{O}$  and  $\text{D}_2\text{O}$  were purchased from Aldrich, and  $\text{CD}_3\text{COOD}$  was purchased from Wako Chemicals. These were used without further purification.

### 3. Results

**3.1. Steady-State Infrared Absorption Spectra.** The steady-state IR absorption spectra of  $\text{CH}_3\text{COOD}$  and  $\text{CD}_3\text{COOD}$  in  $\text{D}_2\text{O}$  were measured with a Fourier-transform IR spectrometer, as shown in Figure 2. An absorption band due to the carbonyl CO stretching vibration was observed at around  $1700\text{ cm}^{-1}$  for both  $\text{CH}_3\text{COOD}$  and  $\text{CD}_3\text{COOD}$ . The absorption band, showing a shoulder on the lower-wavenumber side, could not be fitted by a single Lorentzian or Gaussian function, or their sum. However, the obtained absorption band could be fitted well by

**TABLE 1: Spectroscopic Properties of the Voigt Components of the Carbonyl CO Stretching Vibrational Absorption**

solute	peak position/ $\text{cm}^{-1}$	total width (fwhm)/ $\text{cm}^{-1}$	area ratio <sup>a</sup>
$\text{CH}_3\text{COOD}$	1712.1	30.2	47
	1683.2	35.2	53
$\text{CD}_3\text{COOD}$	1703.0	39.7	56
	1682.4	37.9	44

<sup>a</sup> Ratio of the area intensities obtained by integration of the Voigt components. The sum of the ratios for the two components is 100.

the sum of two Voigt functions, which are a convolution of Gaussian and Lorentzian functions. The peak positions and bandwidths of the Voigt components are summarized in Table 1. This result indicates that the absorption bands are broadened by both homogeneous and inhomogeneous contributions. However, it is difficult to discuss the homogeneous and inhomogeneous widths at a quantitative level, because the obtained bandwidths of the convoluted Gaussian and Lorentzian components contain large uncertainties.

The two Voigt components are located at  $1712$  and  $1683\text{ cm}^{-1}$  for  $\text{CH}_3\text{COOD}$  and at  $1703$  and  $1682\text{ cm}^{-1}$  for  $\text{CD}_3\text{COOD}$ . Their bandwidths are 30 to  $40\text{ cm}^{-1}$ . The peak position and bandwidth of the acetic acid monomer in aprotic solvents, for example,  $\text{CCl}_4$ , *n*-hexane, and benzene, are reported to be  $1760$ – $1780\text{ cm}^{-1}$  and  $12$ – $15\text{ cm}^{-1}$ , respectively.<sup>21,31</sup> The differences of the peak wavenumbers and the bandwidths in  $\text{D}_2\text{O}$  from those of the monomer result from the hydrogen-bonding interactions between the CO group and the solvent water molecules.

We next discuss the origins of the two Voigt components of the IR absorption band. The IR absorption band shape fitted with the sum of the two Voigt functions possibly indicates the presence of two complexes of acetic acid. It has been suggested from UV spectroscopic studies that there are three dominant species of molecular complexes at the concentration of  $0.3\text{ mol dm}^{-3}$ , that is, a complex of neutral acetic acid and two water molecules, a complex of neutral acetic acid and one water molecule, and a complex of an acetic acid anion and two water molecules.<sup>19</sup> The third complex does not contribute to the IR absorption spectrum at around  $1700\text{ cm}^{-1}$ , because the IR absorption band arising from the OCO asymmetric stretching vibration of the anion appears at around  $1600\text{ cm}^{-1}$ . The two Voigt components of the IR absorption band around  $1700\text{ cm}^{-1}$  probably result from the two complexes of neutral acetic acid and water. However, in the steady-state IR study, the band shape of the CO stretching mode of acetic acid in  $\text{D}_2\text{O}$  was interpreted in terms of the Fermi resonance between the CO stretching mode and the overtone of the CC stretching mode.<sup>13</sup> It was also concluded that the difference in the band shape between  $\text{CH}_3\text{COOD}$  and  $\text{CD}_3\text{COOD}$  results from the difference in the CC

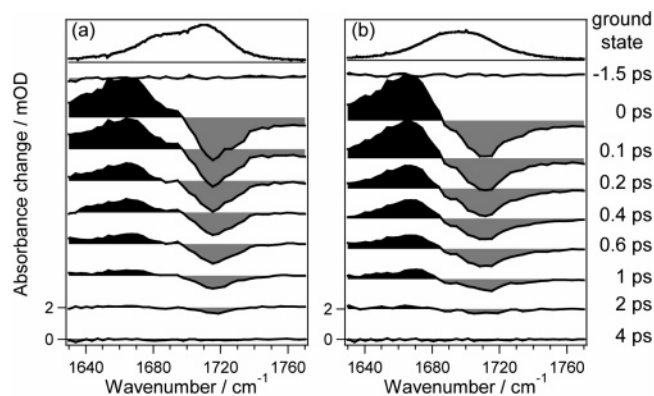


**Figure 3.** Time-resolved IR difference spectra of (a)  $\text{CH}_3\text{COOD}$  and (b)  $\text{CD}_3\text{COOD}$  in  $\text{D}_2\text{O}$ . The top solid line in each spectrum represents the steady-state absorption.

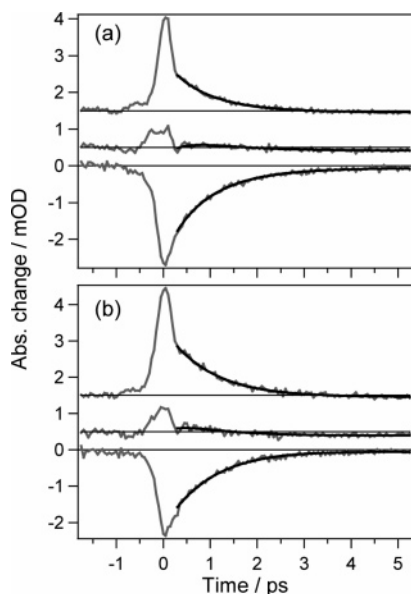


**Figure 4.** Delay time dependences of the absorbance change (gray lines) for (a)  $\text{CH}_3\text{COOD}$  at 1659 (top), 1687 (middle), and 1711 (bottom)  $\text{cm}^{-1}$ , and for (b)  $\text{CD}_3\text{COOD}$  at 1662 (top), 1680 (middle), and 1708 (bottom)  $\text{cm}^{-1}$ . The solid black lines correspond to biexponential functions determined by global fitting.

stretching vibrational frequency,  $850\text{ cm}^{-1}$  for  $\text{CH}_3\text{COOD}$  and  $800\text{ cm}^{-1}$  for  $\text{CD}_3\text{COOD}$ . In section 4.1, we discuss a possible contribution of the Fermi resonance to the band shape in light of the time-resolved IR absorption spectra, and conclude that the Fermi resonance is not important in the IR spectrum.

**3.2. Time-Resolved Infrared Difference Spectra.** We measured the time-resolved difference spectra after vibrational excitation of the CO stretching mode of  $\text{CH}_3\text{COOD}$  and  $\text{CD}_3\text{COOD}$  in  $\text{D}_2\text{O}$ . The results are displayed in Figure 3. The depletion of the ground-state absorption band is observed at  $1711\text{ cm}^{-1}$  for  $\text{CH}_3\text{COOD}$  and at  $1708\text{ cm}^{-1}$  for  $\text{CD}_3\text{COOD}$ , while the transient absorption band due to the transition from the  $\nu = 1$  state to the  $\nu = 2$  state is observed at  $1659\text{ cm}^{-1}$  for  $\text{CH}_3\text{COOD}$  and at  $1662\text{ cm}^{-1}$  for  $\text{CD}_3\text{COOD}$ . The recovery of the depletion and the decay of the transient absorption correspond to the VER process from the  $\nu = 1$  to the  $\nu = 0$  state.

The time profiles of the absorbance change at three wavenumbers,  $1711$ ,  $1687$ , and  $1659\text{ cm}^{-1}$  for  $\text{CH}_3\text{COOD}$  and  $1708$ ,  $1680$ , and  $1662\text{ cm}^{-1}$  for  $\text{CD}_3\text{COOD}$ , are shown in Figure 4. We fitted the time dependences of the signals in the wavenumber

region ranging from  $1625$  to  $1760\text{ cm}^{-1}$  with a biexponential function,

$$\Delta A(\omega, t) = a(\omega) \exp\left(-\frac{t}{\tau_1}\right) + b(\omega) \exp\left(-\frac{t}{\tau_2}\right) + c(\omega) \quad (1)$$

where  $\Delta A(\omega, t)$  is the observed absorbance change at the wavenumber  $\omega$ , with the delay times  $t$ ,  $\tau_1$  and  $\tau_2$  are the decay time constants of the biexponential function,  $a(\omega)$  and  $b(\omega)$  are the decay-associated spectra, and  $c(\omega)$  is the spectrum of the quasi-static component. By applying the global fitting to the time-resolved difference spectra after the delay time of  $300\text{ fs}$ , we have determined the  $\tau_1$  and  $\tau_2$  values as  $450 \pm 200\text{ fs}$  and  $980 \pm 40\text{ fs}$  for  $\text{CH}_3\text{COOD}$  and as  $390 \pm 190\text{ fs}$  and  $930 \pm 40\text{ fs}$  for  $\text{CD}_3\text{COOD}$ , respectively. The spectra  $a(\omega)$ ,  $b(\omega)$ , and  $c(\omega)$  obtained by the fitting are shown in Figure 5.

In ultrafast pump–probe spectroscopy, the signal at the negative time delay originates from the perturbed free induction decay (PFID).<sup>12,32</sup> In addition, the coherent effect, called pump polarization coupling (PPC), is also observed when the pump and probe pulses are temporally overlapped.<sup>12,33</sup> The contributions from the PFID and PPC are negligible in the time region when the pump pulse reaches the sample before the probe pulse. The width of the cross correlation function between the pump and probe pulses is about  $250\text{ fs}$ . Therefore, the signals after the time delay of  $300\text{ fs}$  should not be affected by the coherent effects. We fitted the signal after a delay time of  $300\text{ fs}$  to avoid contributions from the coherent effects, resulting in large uncertainties in the  $\tau_1$  values. However, even when the  $\tau_1$  value is changed in the range of the uncertainty, the shape of the spectrum  $a(\omega)$  is not changed. The uncertainty in the  $\tau_1$  value does not alter the conclusion of this work.

## 4. Discussion

### 4.1. Origins of Decay-Associated Spectra, $a(\omega)$ and $b(\omega)$ .

We have decomposed the observed time-resolved spectra into two dynamical components,  $a(\omega)$  and  $b(\omega)$ , and a quasi-static component  $c(\omega)$ . To elucidate the two components,  $a(\omega)$  and  $b(\omega)$ , we compared the decay-associated spectra with the steady-state absorption spectra. As shown in Table 1, the ground-state absorption band of the CO stretching mode includes two Voigt components whose peak positions are  $1712$  and  $1683\text{ cm}^{-1}$  for  $\text{CH}_3\text{COOD}$  and  $1703$  and  $1682\text{ cm}^{-1}$  for  $\text{CD}_3\text{COOD}$ . The depletions in the spectra  $a(\omega)$  and  $b(\omega)$  exhibit peaks at the wavenumbers of  $1711$  and  $1694\text{ cm}^{-1}$  for  $\text{CH}_3\text{COOD}$  and  $1708$  and  $1680\text{ cm}^{-1}$  for  $\text{CD}_3\text{COOD}$ , respectively. As mentioned in section 3.2, the time constant  $\tau_1$  and the spectrum  $a(\omega)$  include some fitting uncertainties. The difference of the position by  $12\text{ cm}^{-1}$  between the lower-wavenumber Voigt component and the depletion in the spectrum  $a(\omega)$  for  $\text{CH}_3\text{COOD}$  results from these uncertainties. Therefore, we conclude that the band shape and the position of the Voigt component at the lower wavenumber correspond well with those of the depletion in the spectrum  $a(\omega)$ , while the band shape and the position of the higher wavenumber component correspond with those of the depletion in the spectrum  $b(\omega)$  for both  $\text{CH}_3\text{COOD}$  and  $\text{CD}_3\text{COOD}$ . In addition, if the shoulder of the ground-state IR absorption band resulted from the Fermi resonance, the difference of the band shape between  $\text{CH}_3\text{COOD}$  and  $\text{CD}_3\text{COOD}$  would indicate that the contribution from the Fermi resonance is different. A different contribution from the Fermi resonance would lead to differences in the VER time constants. However, the VER time constants,  $\tau_1$  and  $\tau_2$ , are nearly the same for  $\text{CH}_3\text{COOD}$ ,  $450$  and  $980\text{ fs}$ , and  $\text{CD}_3\text{COOD}$ ,  $390$  and  $930\text{ fs}$ . These results suggest that the



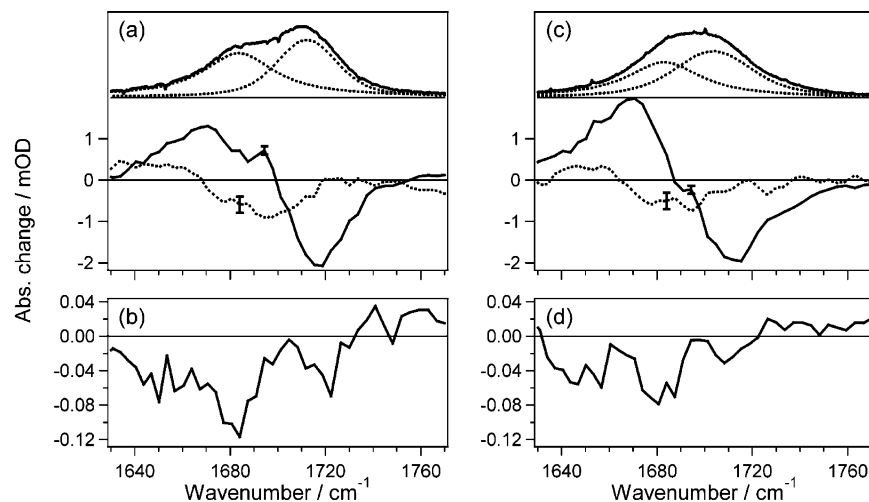


**Figure 5.** Decay-associated spectra obtained by global fitting. (a) Spectra of the 450 fs [ $a(\omega)$ , dotted line] and 980 fs [ $b(\omega)$ , solid line] decaying components for  $\text{CH}_3\text{COOD}$ . The upper traces show the steady-state absorption band (solid line) and the two Voigt components (dotted lines). The uncertainties in the amplitudes are indicated in the figure. (b) Spectrum of the quasi-static component [ $c(\omega)$ ] for  $\text{CH}_3\text{COOD}$ . (c) Spectra of the 390 fs [ $a(\omega)$ , dotted line] and 930 fs [ $b(\omega)$ , solid line] decaying components for  $\text{CD}_3\text{COOD}$ . The upper traces show the steady-state absorption band (solid line) and the two Voigt components (dotted lines). The uncertainties in the amplitudes are indicated in the figure. (d) Spectrum of the quasi-static component [ $c(\omega)$ ] for  $\text{CD}_3\text{COOD}$ .

shape of the ground-state absorption band showing the shoulder is not due to the Fermi resonance but due to the presence of two components. We conclude that the decay-associated spectra  $a(\omega)$  and  $b(\omega)$  result from the excitation of the lower and higher wavenumber Voigt components, respectively. It is also concluded that the exchange between the components with the spectrum  $a(\omega)$  and those with the spectrum  $b(\omega)$  proceeds slower than the VER process with the time constant of 1 ps.

The evolution of the time-resolved spectrum could be explained by other mechanisms of vibrational dynamics. Spectral diffusion, observed in the OH stretching dynamics of HOD in  $\text{D}_2\text{O}$ ,<sup>34,35</sup> could be considered as the origin of the decay-associated spectrum  $a(\omega)$  or  $b(\omega)$ . The ground-state absorption band fitted with the sum of the two Voigt functions indicates the presence of the inhomogeneous distribution of the transition frequency which may result in the spectral diffusion. Under our experimental conditions, the two Voigt components were excited simultaneously by the IR pump pulse with a spectral width of  $160\text{ cm}^{-1}$ , which covers the entire range of the IR absorption band of the CO stretching mode. Therefore, spectral diffusion caused by fast exchange between the two components should not be observed. The Stokes shift in the vibrational excited state is another possible mechanism of spectral diffusion because the two components in the ground-state absorption band include the homogeneous and inhomogeneous contributions as discussed in section 3.1. However, the depletion of the ground-state absorption and the transient absorption bands do not exhibit any wavenumber shift during the delay time. Their widths are also not changed. It is concluded that spectral diffusion is not important in the present results. As another interpretation for the spectral time evolution, the slower component could result from an intermediate hot ground state formed by the VER from the  $\nu = 1$  state. However, this mechanism is also unlikely because of the agreement of the wavenumbers between the slower component and the lower frequency Voigt component.

The two components of  $\text{CH}_3\text{COOD}$  and  $\text{CD}_3\text{COOD}$  probably correspond to different solvation complexes in  $\text{D}_2\text{O}$ . When the concentration is changed in the range lower than  $1\text{ mol dm}^{-3}$ , the shapes of the steady-state IR and Raman spectra do not depend on the concentration.<sup>13,18</sup> The results indicate that acetic acid molecules do not form hydrogen bonds with each other. It

has also been suggested from UV spectroscopic studies that there are two complexes of neutral acetic acid forming hydrogen bonds with one (1:1 complex) or two (1:2 complex) water molecules when the concentration is  $0.3\text{ mol dm}^{-3}$ .<sup>19</sup> Therefore, we conclude that the lower wavenumber Voigt component is attributed to the 1:2 complex, while the higher wavenumber Voigt component is attributed to the 1:1 complex. The exchange between the 1:2 and the 1:1 complexes by hydrogen bond breaking or forming proceeds with a time constant of larger than 1 ps, as discussed in section 4.1. In the two-dimensional (2D) IR spectroscopic study on *N*-methylacetamide in methanol, it was suggested that the hydrogen bond between the carbonyl group of *N*-methylacetamide and methanol breaks and forms with a time constant from 10 to 15 ps.<sup>36</sup> The time scale of the hydrogen bond breaking and forming between the carbonyl group of acetic acid and  $\text{D}_2\text{O}$  seems to correspond with that between the carbonyl group of *N*-methylacetamide and methanol. In future studies, if a spectrally narrower IR pulse is used as the pump and its peak position is tuned to the wavenumber of either of the two components, the pump-probe signal should provide more information on the vibrational dynamics, such as the spectral diffusion and the exchange between the two species.

To support our spectral assignments, we performed calculations of the density functional theory for the 1:1 complexes ( $\text{CH}_3\text{COOD}-\text{D}_2\text{O}$  and  $\text{CD}_3\text{COOD}-\text{D}_2\text{O}$ ) and the 1:2 complexes [ $\text{CH}_3\text{COOD}-(\text{D}_2\text{O})_2$  and  $\text{CD}_3\text{COOD}-(\text{D}_2\text{O})_2$ ] with the Gaussian 03 program.<sup>37</sup> The calculations were performed by the B3LYP functional with a 6-311+G(d,p) basis set. The wavenumbers of the CO stretching vibrations for  $\text{CH}_3\text{COOD}$ , the 1:1 complex ( $\text{CH}_3\text{COOD}-\text{D}_2\text{O}$ ) and the 1:2 complex [ $\text{CH}_3\text{COOD}-(\text{D}_2\text{O})_2$ ] were calculated as 1766, 1712, and  $1682\text{ cm}^{-1}$ , respectively, after the frequency correction by the wavenumber-linear scaling method.<sup>38</sup> The wavenumbers for the 1:1 and 1:2 complexes of  $\text{CH}_3\text{COOD}$  agree well with the peak positions of the Voigt components in the steady-state absorption spectrum, 1712 and  $1683\text{ cm}^{-1}$ , respectively. For  $\text{CD}_3\text{COOD}$ , the calculated wavenumbers for the 1:1 and 1:2 complexes are 1707 and  $1676\text{ cm}^{-1}$ , agreeing with the peak positions of the Voigt components, 1703 and  $1682\text{ cm}^{-1}$ , respectively. These results support our spectral assignments.

**4.2. Mechanism of Vibrational Energy Relaxation of Acetic Acid in Aqueous Solution.** We discuss the VER time constants,  $\tau_1$  and  $\tau_2$ , of the CO stretching mode of acetic acid in D<sub>2</sub>O. As discussed in section 4.1, the  $\tau_1$  value, 400 fs, corresponds to the VER time for the 1:2 complex, while the  $\tau_2$  value, 1 ps, corresponds to that for the 1:1 complex. The VER process of the CO stretching mode for the 1:2 complex proceeds faster than that for the 1:1 complex. It has been observed that the stronger intermolecular hydrogen bond accelerates the VER process of the OH stretching mode of HOD in D<sub>2</sub>O.<sup>39–41</sup> The VER rate is formulated in terms of the Fermi golden rule, in which the VER rate becomes slower when the coupling strength between the excited vibrational mode and the energy accepting mode increases, the vibrational density of states (DOS) increases, and the energy gap between the excited vibrational mode and the energy accepting mode decreases. When a hydrogen bond is formed, the vibrational DOS at the wavenumber of the CO stretching vibration greatly increases because of a combination of the low-frequency modes from the hydrogen bond and the intramolecular vibrational modes. The DOS of the 1:2 complex is, therefore, larger than that of the 1:1 complex, leading to the faster VER process for the 1:2 complex. On the other hand, the vibrational frequency of the CO stretching mode of acetic acid decreases by the formation of the hydrogen bond. It is also possible that the difference of the VER rate between the 1:2 complex and the 1:1 complex results from a different energy gap between the excited vibrational mode and the energy accepting mode. Further investigation is needed to clarify which is the major factor contributing to the acceleration of the VER process by the formation of an extra hydrogen bond in the 1:2 complex.

We discuss the two time constants,  $\tau_1$  and  $\tau_2$ , for CH<sub>3</sub>COOD and CD<sub>3</sub>COOD. The values of  $\tau_1$  and  $\tau_2$  are identical between CH<sub>3</sub>COOD and CD<sub>3</sub>COOD within experimental uncertainties. The frequencies of the bending, rocking, and twisting modes of the methyl group are decreased by the deuteration.<sup>13</sup> Although the frequency shifts may change the efficiency of the energy transfer from the CO stretching vibration to the vibrations related to the methyl group, the experimental results indicate that the VER time is not different between CH<sub>3</sub>COOD and CD<sub>3</sub>COOD. It should be noted that the VER process of the OD stretching mode of C<sub>6</sub>H<sub>5</sub>OD in chloroform is accelerated by the increase of the hydrogen bond strength up to a certain limiting rate.<sup>42</sup> If the VER rate reached this limit, a difference in the VER rate would not be observed between CH<sub>3</sub>COOD and CD<sub>3</sub>COOD. However, as we discussed, the VER time for the 1:2 complex,  $\tau_1 = 400$  fs, is shorter than that for the 1:1 complex,  $\tau_2 = 1$  ps. The VER rate for the 1:1 complex has, at least, not yet reached the limiting rate if there is a limiting rate for this system. Therefore, the intramolecular vibrational energy transfer from the carbonyl group to the methyl group does not contribute to the dissipation of the vibrational energy deposited to the CO stretching mode. We conclude that the excess energy deposited to the CO stretching mode is distributed among the kinetic degrees of freedom not related to the modes of the methyl group in the first energy dissipation process. The excess vibrational energy should be distributed among the vibrational combination modes or the overtone modes localized in the CCOOD group, or both. The overtone of the CC stretching vibration with its frequency of about 850 cm<sup>-1</sup> is most likely the energy accepting mode.<sup>13</sup>

We next compare the present results to the previous time-resolved IR spectroscopic studies on the acetic acid dimer in CCl<sub>4</sub>. The VER process of the CO stretching mode of the CH<sub>3</sub>-

COOD dimer consists of two steps with time constants of 0.31 and 1.9 ps.<sup>21</sup> It was suggested that the two components resulted from different solvation species. Our experimental results for acetic acid in dilute D<sub>2</sub>O solution also involves two dynamical components, which were assigned to the VER process for the different complexes. These results suggest that the dephasing process proceeds faster than the VER process for the complexes of acetic acid and D<sub>2</sub>O. The differences in the VER time constants, 0.31 and 1.9 ps for the cyclic dimer and 0.4 and 1.0 ps for the complexes of acetic acid and D<sub>2</sub>O, probably result from the different environments of the carbonyl group, including the hydrogen bond strength and the solute–solvent interactions.

**4.3. Origin of Quasi-Static Component,  $c(\omega)$ .** The spectrum  $c(\omega)$  shows a weak bleaching of the steady-state absorption band of the CO stretching vibration, lasting longer than ten picoseconds after the vibrational excitation. In the IR pump–probe spectroscopic studies on the acetic acid cyclic dimer in CCl<sub>4</sub>,<sup>22–26</sup> a depletion of the ground-state absorption band and an absorption increase in the higher wavenumber region after the vibrational excitation of the OH stretching mode are observed. Also, after the excitation of the OH bending mode, the depletion of the ground-state absorption band and the absorption increase at the lower wavenumber region are observed.<sup>24</sup> The signals decayed with a time constant of more than 15 ps. The long-living component was attributed to hydrogen bond weakening due to an increase of the local temperature after the energy dispersion from the first excited vibrational mode.<sup>22–26</sup> Under the present experimental conditions, the carbonyl group also forms hydrogen bonds with the surrounding D<sub>2</sub>O molecules. The slow decay component  $c(\omega)$  is attributed to local heating by dispersed energy from the CO stretching vibration. The decay of the component  $c(\omega)$  may correspond to the cooling process from the locally heated environment.

## 5. Conclusion

The vibrational population dynamics of the carbonyl CO stretching mode of acetic acid has been studied by frequency-resolved IR pump–probe spectroscopy. The time evolution of the difference spectra was interpreted by global fitting analysis with a biexponential function. We obtained two decay-associated spectra and one quasi-static spectrum. The decay-associated spectra show bleaching at lower and higher wavenumbers decaying with the time constants of 400 fs and 1 ps, respectively. These time constants are nearly the same for CH<sub>3</sub>COOD and CD<sub>3</sub>COOD. The excess vibrational energy deposited to the CO stretching mode is first distributed in the CCOOD moiety. The band shape and position of the two components correspond well with those of the two Voigt components in the steady-state absorption band. Two complexes of acetic acid in D<sub>2</sub>O, that is, the 1:1 and 1:2 complexes, are separated dynamically and spectrally.

**Acknowledgment.** This work was partly supported by a Grant-in-Aid (17685001) from the Japan Society for the Promotion of Science.

## References and Notes

- (1) Li, M.; Owrutsky, J.; Sarisky, M.; Culver, J. P.; Yodh, A.; Hochstrasser, R. M. *J. Chem. Phys.* **1993**, *98*, 5499.
- (2) Hamm, P.; Lim, M.; Hochstrasser, R. M. *J. Chem. Phys.* **1997**, *107*, 10523.
- (3) Zhong, Q.; Baronavski, A. P.; Owrutsky, J. C. *J. Chem. Phys.* **2003**, *118*, 7074.
- (4) Zhong, Q.; Baronavski, A. P.; Owrutsky, J. C. *J. Chem. Phys.* **2003**, *119*, 9171.

- (5) Sando, G. M.; Zhong, Q.; Owrutsky, J. C. *J. Chem. Phys.* **2004**, *121*, 2158.
- (6) Sando, G. M.; Dahl, K.; Owrutsky, J. C. *J. Phys. Chem. A* **2004**, *108*, 11209.
- (7) Ohta, K.; Maekawa, H.; Tominaga, K. *J. Phys. Chem. A* **2004**, *108*, 1333.
- (8) Ohta, K.; Maekawa, H.; Tominaga, K. *Chem. Phys. Lett.* **2004**, *386*, 32.
- (9) Ohta, K.; Tominaga, K. *Bull. Chem. Soc. Jpn.* **2005**, *78*, 1581.
- (10) Ohta, K.; Tominaga, K. *Chem. Phys. Lett.* **2006**, *429*, 136.
- (11) Lenchenkov, V.; She, C.; Lian, T. *J. Phys. Chem. B* **2006**, *110*, 1990.
- (12) Hamm, P.; Lim, M.; Hochstrasser, R. M. *J. Phys. Chem. B* **1998**, *102*, 6123.
- (13) Genin, F.; Quiles, F.; Burneau, A. *Phys. Chem. Chem. Phys.* **2001**, *3*, 932.
- (14) Chang, H. C.; Jiang, J. C.; Lin, M. S.; Kao, H. E.; Feng, C. M.; Huang, Y. C.; Lin, S. H. *J. Chem. Phys.* **2002**, *117*, 3799.
- (15) Ng, J. B.; Shurvell, H. F. *J. Phys. Chem.* **1987**, *91*, 496.
- (16) Ng, J. B.; Petelenz, B.; Shurvell, H. F. *Can. J. Chem.* **1988**, *66*, 1912.
- (17) Kosugi, K.; Nakabayashi, T.; Nishi, N. *Chem. Phys. Lett.* **1998**, *291*, 253.
- (18) Nishi, N.; Nakabayashi, T.; Kosugi, K. *J. Phys. Chem. A* **1999**, *103*, 10851.
- (19) Ruderman, G.; Caffarena, E. R.; Mogilner, I. G.; Tolosa, E. J. *J. Solution Chem.* **1998**, *27*, 935.
- (20) Nakabayashi, T.; Sato, H.; Hirata, F.; Nishi, N. *J. Phys. Chem. A* **2001**, *105*, 245.
- (21) Lim, M.; Hochstrasser, R. M. *J. Chem. Phys.* **2001**, *115*, 7629.
- (22) Seifert, G.; Patzlaff, T.; Graener, H. *Chem. Phys. Lett.* **2001**, *333*, 248.
- (23) Heyne, K.; Huse, N.; Nibbering, E. T. J.; Elsaesser, T. *Chem. Phys. Lett.* **2003**, *369*, 591.
- (24) Heyne, K.; Huse, N.; Nibbering, E. T. J.; Elsaesser, T. *Chem. Phys. Lett.* **2003**, *382*, 19.
- (25) Heyne, K.; Huse, N.; Dreyer, J.; Nibbering, E. T. J.; Elsaesser, T.; Mukamel, S. *J. Chem. Phys.* **2004**, *121*, 902.
- (26) Nibbering, E. T. J.; Elsaesser, T. *Chem. Rev.* **2004**, *104*, 1887.
- (27) Huse, N.; Heyne, K.; Dreyer, J.; Nibbering, E. T. J.; Elsaesser, T. *Phys. Rev. Lett.* **2003**, *91*, 197401.
- (28) Huse, N.; Bruner, B. D.; Cowan, M. L.; Dreyer, J.; Nibbering, E. T. J.; Miller, R. J. D.; Elsaesser, T. *Phys. Rev. Lett.* **2005**, *95*, 147402.
- (29) Dreyer, J. *J. Chem. Phys.* **2005**, *122*, 184306.
- (30) Hamm, P.; Kaindl, R. A.; Stenger, J. *Opt. Lett.* **2000**, *25*, 1798.
- (31) Fujii, Y.; Yamada, H.; Mizuta, M. *J. Phys. Chem.* **1988**, *92*, 6768.
- (32) Hamm, P. *Chem. Phys.* **1995**, *200*, 415.
- (33) Brito Cruz, C. H.; Gordon, J. P.; Becker, P. C.; Fork, R. L.; Shank, C. V. *IEEE J. Quantum Electron.* **1988**, *QE-24*, 261.
- (34) Gale, G. M.; Gallot, G.; Hache, F.; Lascoux, N. *Phys. Rev. Lett.* **1999**, *82*, 1068.
- (35) Woutersen, S.; Bakker, H. J. *Phys. Rev. Lett.* **1999**, *83*, 2077.
- (36) Woutersen, S.; Mu, Y.; Stock, G.; Hamm, P. *Chem. Phys.* **2001**, *266*, 137.
- (37) Frisch, M. J.; Trucks, G. W.; Schlegel, H. B.; Scuseria, G. E.; Robb, M. A.; Cheeseman, J. R.; Montgomery, J. A., Jr.; Vreven, T.; Kudin, K. N.; Burant, J. C.; Millam, J. M.; Iyengar, S. S.; Tomasi, J.; Barone, V.; Mennucci, B.; Cossi, M.; Scalmani, G.; Rega, N.; Petersson, G. A.; Nakatsuji, H.; Hada, M.; Ehara, M.; Toyota, K.; Fukuda, R.; Hasegawa, J.; Ishida, M.; Nakajima, T.; Honda, Y.; Kitao, O.; Nakai, H.; Klene, M.; Li, X.; Knox, J. E.; Hratchian, H. P.; Cross, J. B.; Adamo, C.; Jaramillo, J.; Gomperts, R.; Stratmann, R. E.; Yazyev, O.; Austin, A. J.; Cammi, R.; Pomelli, C.; Ochterski, J. W.; Ayala, P. Y.; Morokuma, K.; Voth, G. A.; Salvador, P.; Dannenberg, J. J.; Zakrzewski, V. G.; Dapprich, S.; Daniels, A. D.; Strain, M. C.; Farkas, O.; Malick, D. K.; Rabuck, A. D.; Raghavachari, K.; Foresman, J. B.; Ortiz, J. V.; Cui, Q.; Baboul, A. G.; Clifford, S.; Cioslowski, J.; Stefanov, B. B.; Liu, G.; Liashenko, A.; Piskorz, P.; Komaromi, I.; Martin, R. L.; Fox, D. J.; Keith, T.; Al-Laham, M. A.; Peng, C. Y.; Nanayakkara, A.; Challacombe, M.; Gill, P. M. W.; Johnson, B.; Chen, W.; Wong, M. W.; Gonzalez, C.; Pople, J. A. *Gaussian 03*, Revision B.04; Gaussian, Inc.: Pittsburgh, PA, 2004.
- (38) Yoshida, H.; Takeda, K.; Okamura, J.; Ehara, A.; Matsuura, H. *J. Phys. Chem. A* **2002**, *106*, 3580.
- (39) Woutersen, S.; Emmerichs, U.; Nienhuys, H.-K.; Bakker, H. J. *Phys. Rev. Lett.* **1998**, *81*, 1106.
- (40) Nienhuys, H.-K.; Woutersen, S.; van Santen, R. A.; Bakker, H. J. *J. Chem. Phys.* **1999**, *111*, 1494.
- (41) Wang, Z.; Pakoulev, A.; Pang, Y.; Dlott, D. D. *J. Phys. Chem. A* **2004**, *108*, 9054.
- (42) Rezus, Y. L. A.; Madsen, D.; Bakker, H. J. *J. Chem. Phys.* **2004**, *121*, 10599.